Chapter 3

Animal Models in Exosomes Research: What the Future Holds

Bárbara Adem and Sónia A. Melo

Additional information is available at the end of the chapter

http://dx.doi.org/10.5772/intechopen.69449

Abstract

Exosomes have been implicated in a wide range of pathological and nonpathological processes. Research on tumor-derived exosomes uncovered their role on major processes associated with disease progression. Uncontrolled cellular proliferation resulting in tumor growth, metastatic dissemination and modulation of the immune response, are only a few of the central pathological processes in which tumor-derived exosomes have been implicated. These *in vivo* studies rely on the administration of purified labeled exosomes from cell culture supernatants into circulation of animals or injections of genetically engineered cells that produce labeled exosomes. However, it is not clear that current available techniques actually translate the *in vivo* implications of exosomes in several biological processes. The variations seen when using different exosomes cell sources, the total amount of exosomes injected in mice and their route of administration as well as the fact that most studies are performed in immunodeficient animals, shows the difficulty to achieve conclusions which are biologically significant. Genetically engineered mouse models (GEMM) could be a promising approach to address the current technical limitations allowing tracing tumor-derived exosomes in a living organism. These models could enhance greatly our knowledge about exosomes in different fields of research, namely cancer.

Keywords: exosomes, biodistribution, labeling, *in vivo* imaging, tumor progression

1. Introduction

During the last decades, extensive research on exosomes has contributed to the increasing knowledge on their composition, biogenesis and biological function [1]. Exosomes intrinsic ability of horizontal cargo transfer, and their high stability in circulation, allows them to interact with neighbor and distant cells and phenotypically reprogram them, being important

mediators of cell-to-cell communication [2]. Numerous *in vitro* studies clearly demonstrate exosomes ability to modulate recipient cells through the transfer of their cargo, which includes proteins, DNA and RNA [3–7]. Much effort has been made to evaluate exosomes biological significance *in vivo* through the study of how they flow inside a multicellular organism, their fate upon exocytosis and in which cells they enter and what changes they elicit. Various

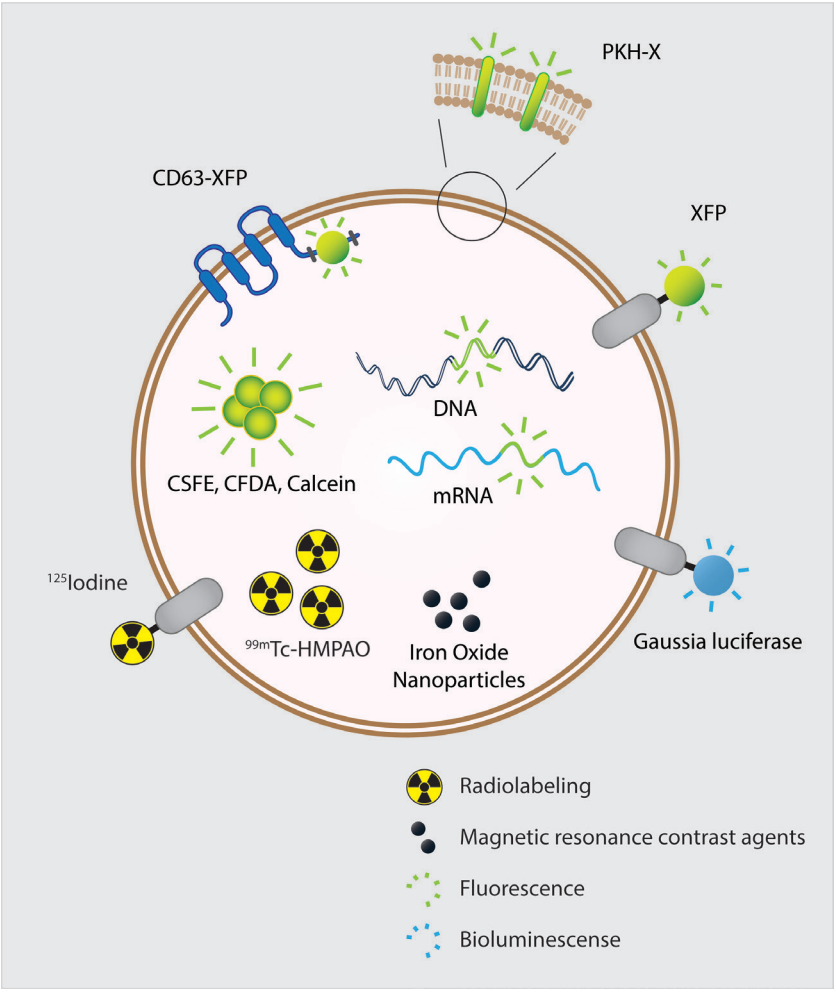

Figure 1. Exosomes biodistribution studies are based on two main approaches: administration of labeled exosomes into circulation of animals, previously extracted from cell culture supernatants, or injections of genetically engineered cells that produce labeled exosomes. Most of the studies performed thus far make use of exogenously produced exosomes isolated from cell culture medium, following injection by different routes of administration, including intraperitoneal (i.p.), intravenous (i.v.), subcutaneous (s.c.), retro-orbital, intranasal and *via* footpad to further track exosomes fate *in vivo*. The other approach consists of injecting subcutaneously or orthotopically cells that had been genetically engineered in order to produce labeled exosomes. This last method allows the track of both cells and corresponding exosomes within the tumor microenvironment or at distant sites.

studies have tried several imaging techniques to track exosomes fate *in vivo* in order to dissect communication routes and their biological implications. Studies conducted so far have described a central role for exosomes in the establishment of the pre-metastatic niche, as well as their close interaction with the immune system [8–12]. Despite latest findings, understanding their spatio-temporal distribution and physiological functions *in vivo* remains a major challenge in the field. Actually, the biological functions of exosomes *in vivo*, including tissue distribution, blood levels and clearance dynamics remain largely unexplored.

Exosomes biodistribution research is based on two main approaches: administration of purified labeled exosomes from cell culture supernatants into circulation of animals or injections of genetically engineered cells that produce labeled exosomes (**Figure 1**). According to the literature, most studies performed so far used exogenously produced exosomes isolated from cell culture medium, following treatment using different routes of administration, including intraperitoneal (i.p.), intravenous (i.v.), subcutaneous (s.c.), retro-orbital, intranasal and *via* footpad to further track exosomes fate *in vivo* [10, 13–15]. To successfully follow exosomes

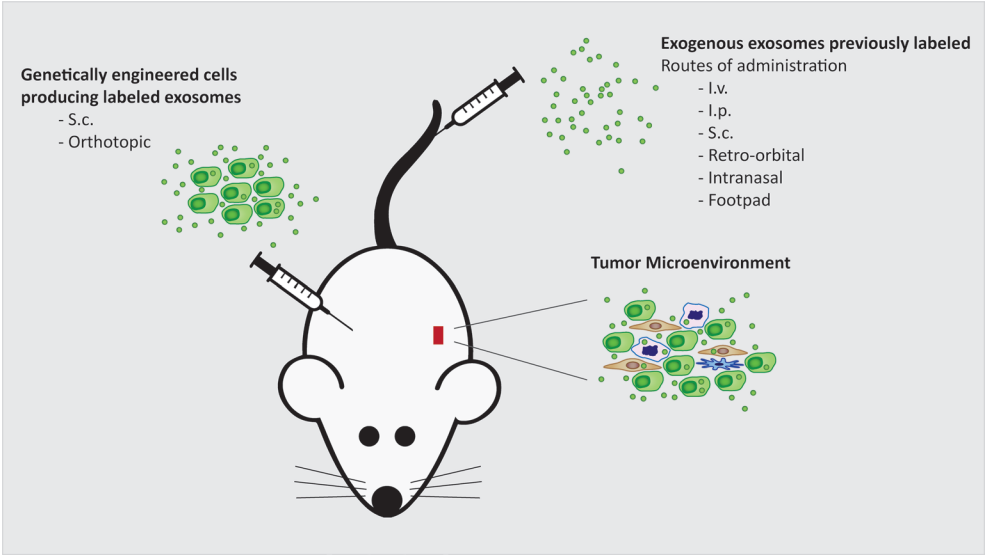

Figure 2. Different methods available to label exosomes. Fluorescent labeling of exosomes is the most widely used method to trace their fate *in vivo*. Membrane-intercalating fluorescent dyes such as PKH or PKH26 are very common. Fluorescent probes labeling DNA, mRNA and proteins contained in exosomes are also an option. Additionally, membrane permeable fluorescent dyes as carboxyfluorescein succinimidyl ester (CFSE), 5(6)-carboxyfluorescein diacetate (CFDA) and calcein fluoresce as a consequence of esterification. Furthermore, exosomes labeling resulting of the genetic engineering of the cells of origin are also a common approach. Fluorescent reporters can be fused to exosomes markers like CD63. Fluorescent labeling can be detected using standard optical imaging techniques. Other labeling systems have been developed such as the bioluminescence reporters like gaussia luciferase fused to transmembrane domains of known proteins like lactadherin or platelet-derived growth factor receptor. Other options include radiolabeling of exosomes using ^{125}Iodine to label exosomal proteins located on the outer membrane or by using ^{99m}Tc-hexamethylpropyleneamineo (HMPAO) that can be visualized using single-photon emission computed tomography. Exosomes labeling with magnetic resonance contrast agents such as iron oxide nanoparticles is an innovative approach and further tracking can be achieved through magnetic resonance imaging.

fate *in vivo*, labeling methods should satisfy the following requirements: (1) specifically label exosomes rather than extracellular vesicles (EVs) in general; (2) be stable and accumulate sufficient signal to detect exosomes from background noise; (3) not interfere with exosomes natural half-life; and (4) not alter exosomes properties. Taking these into consideration, several methods have been developed to labels EVs, namely exosomes (**Figure 2**).

2. Bioluminescence reporter system

Genetically engineered bioluminescent proteins such as Gaussia luciferase, combined with transmembrane domains like lactadherin- or platelet-derived growth factor receptor (PDGFR), could reveal the spatiotemporal distribution of EVs in a quantitative manner in small animals [14, 16]. This approach overcomes the limitation of background auto-fluorescence when working with fluorescent proteins. Nevertheless, this system presents the disadvantage of attenuated signal when located in a deep organ. In 2013, Takahashi et al. designed a new reporter system based on bioluminescence that enables tissue biodistribution and pharmacokinetic studies [16]. This system is based on a fusion protein comprising Gaussia luciferase (gLuc) and a N-terminal secretion signal of lactadherin and C1C2 domains of lactadherin. The gLuc is a reporter protein that emits a very strong chemiluminescent signal when its substrate, coelenterazine (CTZ), is present, while lactadherin is a membrane-associated protein mainly found in exosomes [17, 18]. N-terminal secretion signal of lactadherin was found to be necessary for the protein to be transported to exosomal compartments and C1C2 domains necessary for its retention on exosomes membrane [18]. Exosomes derived from B16-BL6 murine melanoma cells transfected with GLuc lactadherine (GL exosomes) were collected and then used to intravenously inject mice. GL exosomes were administered on Balb/c mice *via* tail vein, and their distribution was evaluated by *in vivo* imaging. While in the first hour, chemioluminescence was mainly detected in the liver and the lungs, 4 h post-injection, a strong signal was only detected in the lungs. Interestingly, the authors injected PKH26 labeled exosomes derived from nontransfected B16-BL6 cells into mice and concluded that the biodistribution pattern was similar when they used GL exosomes, which suggests that this reporter hardly changes the biodistribution pattern of B16-BL6 exosomes. GL exosomes pharmacokinetic, upon tail vein injection into C57/BL6 mice, showed a half-life of approximately 2 min, and less than 5% remained in the serum after 5 min upon the i.v. injection. At 4 h upon injection, strong gLuc activity was detected in the lungs and spleen [16]. Further studies developed by the same group investigated the clearance mechanism of i.v. injected B16BL6 GL exosomes [19]. PKH26-labeled B16BL6 exosomes were taken up by macrophages present in the liver and spleen and by endothelial cells in the lung. To assess the role of macrophages in exosomes clearance, B16BL6 GL exosomes were i.v. injected into macrophage-depleted mice. In those animals, exosomes clearance was significantly delayed, and levels were reduced to around 1.6% comparing to the untreated mice. Collectively, these findings demonstrate that macrophages play a preponderant role in the clearance of injected exosomes from the blood circulation.

Lai et al. also developed an additional multimodal reporter for EVs imaging based on bioluminescence [14]. A recombinant protein composed of a transmembrane domain of PDGFR

fused to a biotin acceptor domain that is fused to the humanized Gaussia luciferase was expressed in the membranes of EVs. In the presence of coelenterazine (CTZ), the purified vesicles exhibited a strong bioluminescent signal. When conjugated to streptavidin-Alexa 680, the EVs can be imaged *in vivo* noninvasively using several techniques: magnetic resonance imaging (MRI), single-photon emission computed tomography/positron emission tomography (SPEC/PET) and fluorescence-mediated tomography (FMT). Stable clones of HEK293T cells expressing both the recombinant protein and the humanized biotin ligase were used to collect the modified EV, and to systemically inject in nude mice, upon which their biodistribution and clearance were evaluated. EV-gLucB or Phosphate-buffered saline (PBS) was injected into athymic nude mice *via* the retro-orbital vein. Immediately before imaging, CTZ was administered revealing a great amount of gLuc signal in the spleen and liver in EV-gLucB treated mice when compared to the controls group. To further investigate the multimodals imaging capability, EV-gLucB or PBS was labeled with streptavidin-Alexa 680 conjugate and then injected *via* tail vein into athymic nude mice and imaged 30 min later with FMT. Similarly to the biodistribution seen by gLuc bioluminescence, EVs were found to accumulate mainly in the spleen and liver. To assess biodistribution of i.v. administered EV-gLucB, organs were collected at different time points post-treatment and gLuc activity was analyzed. The highest signal was detected in the spleen, followed by the liver, lungs and kidney, which is in agreement with the *in vivo* results. On the other hand, the brain, heart and muscle showed lower amounts of signal across all time points. Interestingly, EVs signal decreased by more than half from 30 to 60 min in the liver and the kidneys, while during the same period, spleen and lung levels remained constant. In another experiment, EV-treated animals were transcardially perfused with PBS before harvesting the organs at different time points. Notably, perfused kidneys showed the highest EV signal followed by liver, lung, heart, brain, muscle, and finally, the spleen showing the lowest signal amounts across all time points. These findings suggest that cells that compose the spleen, even though high amounts of EVs are present in the blood that supplies this organ, do not efficiently take up EVs. The prevalent EVs localization in the nonperfused spleen is most likely attributed to an excess of EVs dosage resulting in the saturation of liver macrophages, leading to higher levels of EVs in circulation and consequently into spleen vasculature. Other possibility renders from the fact that EVs can be taken up in the blood by macrophages or lymphocytes that travel to the spleen. Perfused liver and lungs displayed similar reduction patterns from 30 to 60 min when compared to the nonperfused scenario indicating that these organs actively take up EVs. A similar trend was found to the brain, heart and muscle demonstrating that these organs take up EVs although in small amounts. Even though the kidneys displayed the highest amounts of vesicles accumulation, authors called our attention to a possible artifact of the perfusion procedure. In this case, EVs present in the blood would be forced into the kidneys. To study EVs kinetics in biofluids, blood and urine were collected at different time points post EV injection, and luciferase activity was evaluated. The maximum signal was detected at 30 min (earliest time point), followed by a quick reduction at 60 min and then a slow decline from 90 to 360 min. In the urine, the highest signal was measured at 60 min followed by a fast decrease from 60 to 120 min and then a progressive decline from 120 to 360 min. Altogether these findings suggest that only a minor part of EV-gLucB is cleared by the renal route upon the distribution phase. At the last time point, baseline signal was detected in the blood, whereas the urine in addition to some organs still showed part of the signal. Finally, in order to study the potential

delivery of EV-gLucB to tumors, athymic nude mice with a subcutaneous human xenograft tumor were injected *via* tail vein with EV-gLucB. One hour post-treatment bioluminescence imaging revealed EV-gLucB accumulation in the tumor. When comparing liver, spleen and tumors gLuc activity, tumors were found to exhibit the highest gLuc levels. Overall, this was the first time a multimodal approach to label EVs was used giving insight into vesicles biodistribution and kinetics.

3. Radiolabeling of exosomes

In 2014, Morishita et al. developed a method to quantitatively assess the biodistribution of B16BL6-derived exosomes using iodine-125 (^{125}I) labeling on a streptavidin (SAV)-biotin system [20]. B16BL6 cells were transfected with a plasmid vector encoding the fusion protein SAV-lacadherin, and the resulting exosomes were purified and incubated with (3-^{125}I-iodobenzoyl) norbiotinamide (^{125}I-IBB) to obtain ^{125}I labeled exosomes. Balb/c mice were i.v. injected with ^{125}I labeled B16BL6 exosomes or control conditions. ^{125}I labeled B16BL6 exosomes first underwent a distribution step with a half-life of 1.5 min and then entered a clearance phase with a half-life of 346 min, indicating that exogenously administered exosomes have short half-lives in circulation. Furthermore, ^{125}I labeled B16BL6 exosomes were found to distribute to the liver, spleen and lung after systemic administration. High levels of radioactivity signal were found in the liver at 1 min, reaching a peak at 30 min and following a decrease at 4 h. Spleen distribution pattern was the same as the liver though at lower levels. Liver and spleen make part of the mononuclear phagocyte system, which is rich in macrophages and potentially responsible for the clearance of exosomes. Notably, at 1 min, a considerable amount of radioactivity was detected in the lungs, which had its peak at 1 h and decreased at 4 h. This can be due to exosomes aggregation possibly through interaction with blood components. Authors concluded that radiolabeling of exosomes with iodine-125 using the SAV-biotin system is a better choice when quantitatively determining exosomes tissue biodistribution than approaches based on fluorescence or chemioluminescence.

Additional methods have been developed to radiolabel exosomes. Hwang et al. produced exosomes-mimetic nanovesicles (ENVs) from extrusion of macrophage cells and radiolabeled them with ^{99m}Tc-hexamethylpropyleneamineo (HMPAO) under physiologic conditions [21]. The conversion of ^{99m}Tc-HMPAO in the hydrophilic form that is confined inside cells is accomplished by intracellular glutathione [22]. Further monitoring of ENVs *in vivo* biodistribution was achieved by using SPECT/CT. Biodistribution results of this particular study are not relevant to the matter reviewed in this chapter since ENVs emerged as an alternative to obtain a greater yield of exosomes in a therapeutic point of view [23]. Later, Varga et al. described a new method for radioisotope labeling of EVs using the previous mentioned ^{99m}Tc-HMPAO complex. Moreover, authors demonstrated this methods applicability for the noninvasive evaluation of the tissue distribution of erythrocyte-derived EVs using SPECT/CT [24]. The ^{99m}Tc-HMPAO complex is known to bind to some amino acids including histidine, methionine and cysteine [25]. Therefore, it was expected that this complex would bind to the surface of EVs since it presents numerous membrane proteins. Interestingly, i.v. injection of ^{99m}Tc-tricarbonyl labeled erythrocyte EVs accumulated mostly in the liver and spleen.

4. Labeling exosomes with magnetic resonance contrast agents

Studies performed by Hood group in 2014 described a new electroporation method to load mouse B16-F10 melanoma-derived exosomes with super-magnetic iron oxide nanoparticles (SPION5) [26]. This study was in agreement with their previous findings demonstrating that melanoma exosomes appear to home to the subcapsular sinus in lymph nodes (LN) [10]. Since a right and left pair of popliteal (PO) and inguinal (IN) lymph nodes drains mouse feet, they serve as sentinel LN for footpad tumors. Authors found that animals treated with SPION5 loaded exosomes exhibited a growth in the cross-sectional area of ipsilateral peripheral LN when compared to pre-treatment with free SPION5, probably due to the activation of inflammatory signaling pathways. Moreover, at the 48-h time point, the accumulation of SPION5 in the ipsilateral node was higher for SPION5 loaded exosomes compared to free SPION5. Furthermore, nodes treated with SPION5 loaded exosomes did not display significant differences in the MRI signal when comparing pre-injection and 1-h post-injection conditions. Altogether, these findings demonstrate that a greater amount of SPION5 accumulates in the ipsilateral LN when distributed by exosomes, and that exosomes need more time to deliver SPION5 to the LN than the trafficking time of free SPION5. These observations suggest that exosomes home and stay trapped in sentinel LN. Contrarily, free SPION5 and liposomes follow an unspecific diffusion throughout the LN system. The predominant subcapsular distribution of exosomes carrying SPION5 was further validated by histological analysis with fluorescence microscopy and transmission electron microscopy (TEM).

In 2016, Busato et al. established a new protocol to label exosomes with ultrasmall superparamagnetic iron oxide nanoparticles (USPIO) [27]. USPIO range in size from 5 to 7 nm and are stable and biocompatible [28]. The authors described a new methodology in which adipose stem cells (ASCs) were directly labeled with USPIO rather than exosomes. ASCs are known to incorporate USPIO as part of the endocytic pathway [29]. Furthermore, other studies reported nanoparticles accumulation inside multivesicular bodies, being consequently incorporated into exosomes [30]. This protocol allows the preservation of the integrity of exosomes membrane, since no electroporation is required. The resulting exosomes were isolated, purified and injected in mice intramuscularly. Histological examination of gastrocnemius confirmed the presence of iron and *in vivo* imaging with MRI revealed to be a successful tool to image exosomes *in vivo* in a noninvasive manner.

5. Fluorescent labeling of exosomes

When administering exogenous preparations of exosomes to assess their biodistribution *in vivo*, they need to be first labeled, which can be achieved by using fluorescence techniques.

5.1. Nucleic acids labeling

The use of fluorescent dyes or fluorescent reporters has been one of the gold standard approaches to label exosomes. In addition to proteins, exosomes have been shown to carry RNA and DNA [31]. Therefore, exosomes can be fluorescently labeled using selective dyes for

those nucleic acids. The SYTO 13 dye is cell permeable and has a high fluorescent yield when bound to DNA or RNA [32]. Other DNA binding dyes include H33342 and Thiazole Orange [33]. Alvarez-Erviti et al. research is one good example of this approach since they detect fluorescent signals in the central nervous system after i.v. injection of exosomes derived from dendritic cells (DC) genetically engineered to express RGV peptide on the membrane and loaded with siRNA fluorescently labeled with Cy-3 dye [34].

5.2. Membrane-intercalating fluorescent dyes

Exosomes labeling can also be achieved by using fluorescent lipid membrane dyes, including the commonly used PKH (PKH67, PKH26), which label cell membranes through the insertion of their aliphatic chains into the lipid bilayer [8, 11, 12]. Rhodamine B also known as R18, DiI, DiO and DiD, in addition to PKH, are other examples of lipophilic fluorescent membrane dyes [35–37]. The carbocyanine dyes, DiI (yellow/red fluorescent) and DiO (green fluorescent), are weakly fluorescent in aqueous solutions but become highly fluorescent and reasonably photo-stable when incorporated into cell membranes particularly, DiR (carbocyanine DiOC18(7)) [33]. A limitation for *in vivo* tracking studies is the fact that fluorescent markers should have an emission peak different from the fluorescence emission of biological tissues, in order to overcome the auto-fluorescence background. Notably, near-infrared (NIR) dyes are optimal for *in vivo* applications since they present a high signal/noise ratio, a negligible auto-fluorescence in the range of 700–900 nm (biological tissues emission), and strong tissue penetration of the NIR light [38]. However, lipophilic dyes labeling presents several limitations. Extensive washing steps are necessary to reduce unspecific signal, which can cause significant exosomes loss. Moreover, it promotes aggregates or micelles and may give rise to *in vivo* artifacts since fluorescent dyes persist in tissues after exosomes degradation. This is because lipid labeling is not exosomes specific and fluorescence might remain in degraded exosomes or other cellular structures, since they have an estimated half-life of several days [39]. Therefore, in long-term studies, the extended half-life of the lipophilic dye may result in the conservation of the fluorescent signal for longer than the exosomes persist itself, inducing false positive results as it was evaluated by Grange et al. in 2014 [40]. Ultimately, they confirmed that to reduce unspecific labeling, cells should be directly labeled with the dye, rather than exosomes. Exosomes could be then collected and further purified for administration [40].

5.3. Membrane permeable fluorescent dyes

Exosomes labeling can be achieved using membrane permeable chemical compounds. These dyes become confined to the cytosolic lumen and fluoresce as a consequence of esterification and include carboxyfluorescein succinimidyl ester (CFSE), 5(6)-carboxyfluorescein diacetate (CFDA) [41]. Another example is the use of calcein AM (an acetoxymethyl derivate of the fluorescent molecule calcein) that is a very good cytoplasmic fluorescent dye, since it attains high fluorescence intensities and exhibits an acceptable persistent labeling, given that it does not covalently link to intracellular molecules [33]. Calcein-labeling strategy is based on a membrane-permeant molecule that is nonfluorescent until it is activated by intra-vesicular enzymes [42]. Upon hydrolysis of the acetoxymethyl ester moieties by esterases, calcein

becomes highly membrane impermeable [42]. The detection of calcein-labeled exosomes through flow cytometry has been already described and its use in some experiments has also been reported [43, 44].

Most of the studies performed to date include the use of membrane-labeled exosomes as described in the following examples. Sun et al., in 2010 administered i.p. fluorescent-labeled exosomes carrying curcumin (an anti-inflammatory agent), collected from EL-4 mouse lymphoma cells [15]. The exosomes accumulated in greater amounts in the liver, lungs, kidneys and spleen 1 h post-treatment. Interestingly, when exosomes were administered through the intranasal route, the distribution pattern was re-directed to the brain and intestines.

In 2011, Hood et al. demonstrated for the first time that exosomes isolated from melanoma cells supernatants induced LN conditioning *in vivo* [10]. DiR-labeled B16-F10 melanoma-derived exosomes were injected in the footpads of albino C57/BL6 mice and liposomes were used as control. Sentinel LN was harvested 48 h post-treatment, and fluorescent signals were evaluated using IVIS. They observed that melanoma exosomes home to the IN node ipsilateral to the injection site, whereas liposomes distributed equally in IN nodes both ipsilateral and contralateral to the site of injection. To assess how melanoma exosomes could influence free melanoma cells distribution within a lymphatic microenvironment during metastasis, three serial injections on the left footpad of mice were made in which the last one was accompanied with one million DiO labeled melanoma cells. Lymphatic distribution pattern of melanoma cells was assessed in the sentinel LN. An increased number of melanoma cells infiltrating located in the periphery of the node when mice were pre-treated with exosomes rather than liposomes. Furthermore, melanoma exosomes lead to an increased gene expression involved in cell recruitment, extracellular matrix remodeling and vascular proliferation factors contributing to a microenvironment within the sentinel nodes that favor melanoma cell homing, trapping and growth.

In 2012, Peinado et al. proposed a new role for melanoma-derived exosomes in which they educate bone marrow (BM) progenitor cells to acquire a pro-metastatic phenotype through MET signaling [8]. First, fluorescently labeled B16-F10 exosomes (using PKH67 dye) to analyze exosomes biodistribution were i.v. administered into naive mice. Exosomes were detected in the blood vessels and organs within 5 min after injection. Twenty-four hours post-treatment, exosomes were no longer found in blood circulation. Instead, exosomes were found in the major organotropic sites for B16-F10 metastasis including interstitium lungs, BM, liver and spleen. Next, B16-F10-derived exosomes were injected 3 times a week for 3 weeks, 7 days after orthotopically injection of B16-F10mCherry cells to assess melanoma-derived exosomes role in primary tumor growth and metastasis. Mice showed lung micro-metastasis at day 19 after tumor cell injection in contrast with the control (synthetic unilamellar liposomes). To evaluate the role of the metastatic potential of the cells of origin, equal amounts of exosomes from highly (B16-F10) or poorly (B16-F1) metastatic melanomas were i.v. injected into mice 3 times a week over 28 days, and then subcutaneously implanted B16-F10 cells expressing luciferase. Injection with B16-F10 exosomes resulted in a higher metastatic burden in the lungs and greater tissue distribution, including bone and brain when compared to mice injected with control particles or with B16-F1 exosomes. Notably, these observations indicate that exosomes content can mediate metastatic potential and organotropism. To further investigate

this hypothesis and taking into consideration the central role of bone marrow-derived cells (BMDCs) in metastatic progression, they postulated whether tumor-derived exosomes could educate BMDCs and affect metastatic development. In a process, they termed bone marrow education, GFP-expressing mice were treated with B16-F10 exosomes 3 times a week for 28 days. Next, lethally irradiated mice were transplanted with the educated bone marrow and the mice were also subcutaneously injected with B16-F10 cells expressing mCherry. By pre-educating BMDCs with exosomes from a highly metastatic cancer cell line, an increase in the metastatic tumor burden and distribution in target tissues was observed, even for tumors with a low metastatic capacity. Overall, this work shows that by educating BMDCs tumor exosomes can regulate tumor metastasis. Further proteomics studies revealed MET as a potential candidate implicated in BM education given its previous described role in migration, invasion, angiogenesis and BM cells mobilization. Indeed, additional studies demonstrated that B16-F10-derived exosomes could transfer MET to BM progenitor cells, this way mediating pro-vasculogenic and metastatic effects (enhanced cell mobilization).

In 2015, Costa-Silva et al. proposed a mechanism in which pancreatic ductal adenocarcinoma (PDAC)-derived exosomes induce liver pre-metastatic niche formation in naive mice [11]. Authors demonstrated that Kupffer cells, macrophages present in the liver, uptake PDAC-derived exosomes, which activates the secretion of transforming growth factor β that in turn stimulates hepatic stellate cells to produce fibronectin. The resulting fibrotic microenvironment was showed to enhance the recruitment of BM-derived macrophages. Furthermore, macrophage migration inhibitory factor (MIF) was highly expressed in PDAC-derived exosomes, and its inhibition resulted in abrogation of liver pre-metastatic niche formation and metastasis. Collectively, these data suggest that PDAC-derived exosomal MIF primes the liver for metastasis.

In addition, Hoshino et al. took a step further in investigating pre-metastatic niche formation and unraveling exosomes organotropism [12]. The authors seek to demonstrate tumor-derived exosomes contribution to the establishment of a permissive microenvironment at future metastatic sites, describing their nonrandom biodistribution patterns. In all experiments performed, the authors use prepared pools of exosomes labeled with PKH dyes. They show that exosomes from mouse and human lung-, liver- and brain-tropic tumor cells fuse preferentially with resident cells at their predicted destination sites to prepare the pre-metastatic niche. Surprisingly, treatment with exosomes from lung-tropic tumor cells was sufficient to redirect the metastasis of bone-tropic tumor cells. Further exosomes proteomic studies revealed distinct integrin expression patterns that differed from tumor cells. They found that exosomes expressing integrin $\alpha v\beta 5$ specifically bind to Kupffer cells, mediating liver tropism, whereas exosomal integrins $\alpha 6\beta 4$ and $\alpha 6\beta 1$ mediated lung metastasis through binding with fibroblasts and epithelial cells. Moreover, when these integrins were blocked a decrease of exosomes uptake as well as metastasis formation was observed. Additionally, exosomes uptake by resident cells at metastatic sites mediated by the previously mentioned integrins was found to induce Src phosphorylation and activate the expression of pro-inflammatory S100 response. Altogether, these findings suggest that exosomal integrins are responsible for the adhesion of exosomes to target cells. Furthermore, this interaction activates, in the recipient cells, signaling pathways

involved in inflammatory responses contributing to the formation of a microenvironment that supports the growth of metastatic cells.

Wen et al. associated exosomes derived from highly metastatic breast cancer cell lines with an increase in the metastatic potential partly due to an immune suppression of the tumor microenvironment [9]. Exosomes isolated from murine breast cancer cell lines (metastatic EO771 and 4T1, nonmetastatic 67NR) were labeled with DiD, a lipid-associating fluorescent dye and i.v. injected into mice. Exosomes biodistribution was evaluated in several organs 24 h post-injection using *in vivo* and *ex vivo* imaging and as control liposomes were used. Exogenously administered exosomes distributed mainly to the lungs irrespectively of the metastatic potential followed by spleen. Interestingly, lung and liver displayed higher signaling of exosomes derived from a nonmetastatic cell line compared to a highly metastatic one 4T1. In addition, regardless of the fact 4T1 breast cancer cells frequently exhibit liver tropism, its exosomes did not follow the same pattern. Additionally, exosomes derived from a nonmetastatic cell line distributed preferentially to the liver and lungs. Cumulatively, these results seem to point to the fact that exosomes not always follow the cells tropism patterns, which contrasts with the previously described findings made by Hoshino et al. Taken together, these data suggest that the biodistribution pattern of exosomes may be influenced by numerous factors including cell source, injection route and the amount administered. Therefore, the lack of well-established protocols to perform exosomes biodistribution studies may affect overall results. Nonetheless, Wen et al. further investigated which cell lineages were taking up exosomes in the lung and spleen. They found that around 14% and 3% of $CD45^+$ cells from the lung and spleen, respectively, were taking up EO771-derived exosomes. The majority were macrophages, $CD11b^+$ myeloid cells and dendritic cells. Nevertheless, this uptake pattern was similar in 4T1 and 67NR-derived exosomes. In addition, mice were injected *via* tail vein with a preparation of tumor-derived exosomes every three days for 30 days in order to evaluate the role of breast cancer-derived exosomes in pre-metastatic niche formation in an experiment similar to the one carried out by Peinado in 2012 [8]. They found that exosomes derived from highly metastatic breast cancer cells contributed to the establishment of a permissive microenvironment that in turn promoted cell metastasis trapping and growth in the lung and liver, which was not observed when using exosomes derived from nonmetastatic cells or liposomes. Moreover, EO771 exosomes accumulation in the lung was shown to promote an immunosuppressive microenvironment. This was observed through the recruitment of $CD11b^+/Ly6C^{med}$ granulocytic myeloid-derived suppressor cells, simultaneous to a decrease in T cell and natural killer cells frequency. Furthermore, EO771 exosomes treatment resulted in increased differentiation of naïve T cells ($CD44^{low}CD62L^{hi}$) to effector T cells ($CD44^{hi}CD62^{low}$). This phenomenon was previously described in other tumor microenvironments where T cells further differentiate into 'exhausted' T cells known to be nonfunctional and express high levels of immune inhibitory receptors contributing to cancer cells escape of the immune surveillance [45]. Wen et al. [9] demonstrated the immune suppressive potential of breast cancer-derived exosomes in promoting the pre-metastatic niche formation.

In 2014, Smyth et al. evaluated the tissue distribution of exosomes derived from breast and prostate cancer cell lines when i.v. administered into healthy or tumor-bearing mice [46]. Exosomes were isolated from cell culture supernatants of 4T1, PC3 and MCF-7 cells. Mice

were inoculated with 4T1 cells in the mammary fat pad (MFP) and 15 days after inoculation they were i.v. injected *via* tail vein with 4T1 exosomes fluorescently labeled with DiR. *In vivo* imaging was performed using IVIS at 1, 8 and 24 h post-injection. At the 24-h time point, mice were sacrificed and organs excised for *ex vivo* imaging. One hour after treatment exosomes distributed primarily to the liver and spleen. To further investigate exosomes biodistribution, PC3 and MCF-7 exosomes were radiolabeled with indium-111 and injected i.v. into nude mice-bearing PC3 tumors or nontumor-bearing nude mice. Blood clearance analysis revealed that 3-h post-injection less than 5% of the injected vesicles remained in circulation. Furthermore, the presence of the tumor did not affect exosomes blood clearance. Overall, biodistribution patterns were analyzed 24 h after treatment and found to be very similar to the 4T1 experiment, with greater accumulation in the liver and spleen, followed by the kidneys when compared to other organs including PC3 tumors. In addition, the biodistribution pattern of PC3 exosomes was basically the same in PC3 tumor-bearing nude mice or nontumor-bearing mice. Next, the authors wanted to assess the influence of the innate immune system on exosomes biodistribution and clearance in tumor-bearing mice. Therefore, they inoculated 4T1 cells in the MFP of Balb/c, nude and NOD.CB17-Prkdcscid/J mice and i.v.-injected 4T1 exosomes. It is important to take into consideration that nude mice suffer from a lack of adaptive immune response, while NOD.CB17-Prkdcscid/J mice suffer from impaired innate immunity including impaired complement activity. 4T1 exosomes in nude and Balb/c mice distributed preferentially to the liver and spleen after 20 min post-injection, with levels remaining unaltered over the course of 2 h, suggesting that the adaptive immune system is not responsible for the clearance of exosomes. Interestingly, NOD.CB17-Prkdcscid/J mice displayed an increase in the accumulation of 4T1 exosomes in the liver and spleen between 20 min and 2 h post-injection. The slower uptake of exosomes by the reticuloendothelial system (RES) in NOD.CB17-Prkdcscid/J mice suggests that the innate immune system, alongside with complement opsonization, contributes to exosomes blood clearance.

Recently, Wiklander et al. established a set of experiments demonstrating that EVs biodistribution is dependent on many factors, including cell source, exosomes concentration and route of administration [13]. They injected 1×10^{10} particles/gram body weight (p/g) *via* tail vein of DiR-labeled EVs isolated from HEK293T cell culture supernatant. To assess their biodistribution, organs were harvested for *ex vivo* imaging 24 h post-injection. Importantly, they performed perfused and nonperfused conditions prior to organs harvesting to confirm whether signaling was coming from organs or was due to the presence of labeled EVs in circulation. In addition, EV-free medium was subject to the same protocol as for EV-DiR labeled to exclude the possibility of monitoring free dye. Interestingly, perfusion did not seem to affect EVs biodistribution and EV-free medium injection resulted in insignificant signal in all organs. EVs derived from HEK293T expressing CD63-EGFP plasmid were also used at a concentration of 2.9×10^{10} (p/g). Twenty-four hours post-injection organs were harvested and analyzed. Signal was found on the parenchyma of the liver and spleen. However, little or no signal was detected in lungs and kidney. Next, they evaluated whether EV biodistribution was EV dose dependent. Therefore, they injected different amounts of DiR-labeled HEK293T EVs (0.25×10^{10}, 1×10^{10} and 1.5×10^{10}). Indeed, a positive correlation between EV dosage and total tissue fluorescence was observed. In addition to this phenomenon, a shift

of the relative distribution of EVs among organs also occurred. Relative liver accumulation decreased sequentially with the initial amount of EVs injected. The authors hypothesized that this decrease could result from the saturation of the mononuclear phagocyte system/RES allowing a more effective evasion of the liver at higher amounts. Since the use of lipophilic dyes is associated with prolonged half-life when compared to the EV, the authors evaluated DiR-labeled HEK293T EVs biodistribution at different time points. EVs distribution pattern kept unchanged during 24-h post-injection. However, major differences registered at the time point of 48 h. Fluorescence signal decreased in heart, gastro-intestinal (GI)-tract and kidneys, while the signal in the pancreas suffered a significant increase. These alterations can be due to a re-distribution of EVs or artifacts, since fluorescence dyes are known to have half-lives of several days. In addition, Wiklander et al. evaluated the distribution outcome when the EVs were administered through different routes. In all cases, 1×10^{10} p/g DiR-labeled EV were injected *via* i.v., i.p. or s.c. Interestingly, the different injection routes were associated with different distribution patterns. I.p. and s.c. injections lead to lower EVs accumulation in the liver and spleen, while increased accumulation was detected in the pancreas and GI tract, contrarily to what it was observed for the i.v. injections. Moreover, i.p. injections resulted in higher total tissue fluorescence, while s.c. injections resulted in the lowest one. Their careful analyses also included the influence of the cell of origin in biodistribution outcomes. Three mouse cell sources were used: a muscle cell line C2C12, a melanoma cell line B16F10 and a primary immature BM-derived dendritic cells (DC). Additionally, xenotransplantation of EVs from rat cells—oligodendrocytes OLN-93—and from cells of human origin—HEK293T and primary human mesenchymal stromal cells (MSC)—were used for cross-species studies. All experiments were performed using 1×10^{10} p/g DiR-labeled-EV administered *via* i.v.. Overall, the distribution pattern from the different mouse cell sources did not vary much with spleen, liver, GI tract and lungs being the greatest accumulation sites. Nevertheless, some significant differences were encountered. For instance, C2C12-derived EVs were highly present at the liver, while in the lung displayed the lowest amount of signal accumulated. B16F10-derived EVs were in turn most frequently accumulated in the GI tract, and DC-derived EVs were highly accumulated in the spleen when compared to the other mouse cell sources. Notably, *in vivo* biodistribution patterns did not differ when xenotransplanted EVs were used. MSC-derived EVs displayed higher accumulation in the liver, while the GI tract was the lowest compared to EVs derived from HEK293T and OLN-93 cells. Interestingly, HEK293T, OLN-93 and C2C12 derived EVs presented similar tissue distribution outcomes suggesting that species of origins does not seem to affect the patterns observed. Finally, HEK293T-derived EVs were found to accumulate greatly in the liver and spleen in B16F10 tumor-bearing mice, 24 h post-injection with 1×10^{10} p/g DiR-labeled EV administered *via* i.v., with only 3% of the total fluorescence being detected in the tumor. Wicklander elegantly showed for the first time the different confounders added to EVs *in vivo* biodistribution studies, highlighting the urgency to develop new reliable models.

Another method consists on the genetic engineering of cells to direct the expression of fluorescent markers to the exosomal membrane resulting in labeled exosomes production. Exosomes can be isolated from these cells culture supernatants or cells can be directly injected into mice. One commonly used example is the GFP-CD63 construct. The CD63 is a tetraspanin, a

membrane-associated protein and is known as a general marker of exosomes [47]. Suetsugu and collaborators were one of the first ones to orthotopically inject stable expressing GFP-tagged CD63 cells [48]. They demonstrated that tumor-derived exosomes serve as a central mediators for communication not only between cancer cells but also with their microenvironment components. They produced mouse breast cancer cells (MMT) and human breast cancer cells (MDA-MD-231) RFP labeled stably expressing GFP-tagged CD63 (MMT-RFP/GFP-Exo and MDA-MD-231-RFP/GFP-Exo, respectively). Hence, cells were red and producing green exosomes. To generate orthotopic mouse models of breast cancer metastasis to the lung, they orthotopically injected MMT-RFP/GFP-Exo or MDA-MD-231-RFP/GFP-Exo cells into the MFP of nude mice. Overall, using confocal laser scan microscopy (CLSM), they observed that both in primary tumors and in lung metastasis breast cancer cells secreted exosomes into the tumor microenvironment. To confirm GFP exosomes integration in mice host cells, RFP nude mice were orthotopically injected with the cells previously mentioned into the MFP. GFP-labeled exosomes were taken up by stromal cells namely fibroblasts. Finally, blood samples analysis by CLSM confirmed the presence of GFP exosomes in circulation of mice-bearing lung metastasis.

Nonetheless, when designing these fusion plasmids, one should consider the influence they may have in the protein normal functions. Interestingly, it has been shown that GFP fusion to the N- or C-terminus of CD63 influences protein distribution in rat basophilic leukemia (RBL) cells [49]. When GFP was linked to the C-terminus of CD63 (CD63-GFP), the fused proteins were expressed on both the granule membranes and plasma membranes of RBL cells as native CD63 proteins. Contrarily, when the GFP was conjugated to the N-terminus of CD63 (GFP-CD63), it was homogeneously distributed in the cytoplasm, not being present on granules or the plasma membrane [49]. These results suggested the possibility that the N-terminus of CD63 might play an important role in the establishment of protein localization.

Other approaches developed by Lai et al. in 2014 included a multiplex reporter system consisting of enhanced (EGFP) and tandem dimer tomato (tdTomato) fluorescent proteins fused at NH2-termini with specific palmitoylation signals, enabling EV membrane labeling [39]. By treating cells with EVs carrying fluorescently labeled siRNA, they observed EVs uptake in donor cells. Notably, by combining fluorescent and bioluminescent EVs membrane reporters, they elegantly demonstrated EVs uptake and translation of nascent EV-derived cargo mRNAs in cancer cells *in vitro* as early as 1 h after exposing cells to EVs.

Recently, a new approach was put forward that allows the study of the function of transfer of EVs *in vitro* and *in vivo* settings without the requirement to artificially expose cells to isolated and concentrated pools of EVs [50]. To study the exchange of EVs, the Cre-loxP system was used to fluorescently label Cre-reporter cells that take up the EVs released from cells that express Cre recombinase. Donor cells expressing Cre recombinase were CFP positive (blue), whereas unrecombined Cre-reporter cells were DsRed positive (red) and those that have internalized the EV and have recombined switch from red to green. They demonstrated that the switch in color was due to Cre mRNA containing EVs and not by other mechanisms including free Cre mRNA or protein. Using this technology, they were able to assess whether different types of nontumor cells take up tumor-released EVs [51]. Cre-expressing B16 melanoma cells

were injected into mice ubiquitously expressing the Cre-LoxP reporter tdTomato (tdTomato B6 mice). Notably, nontumor cells expressing tdTomato were found in all analyzed tissues (tumors, lymph nodes, lungs and spleens). This pool of cells presented either $CD45^-$ or $CD45^+$ cells (a general immune cell marker), suggesting that both non-immune cells and immune cells took up tumor-released EVs. By immunohistochemistry, they found that some of those cells were neutrophils and macrophages using different markers. Therefore, authors concluded that tumor cell-derived EVs are taken up by both tumor cells and different sorts of nontumor cells. They next assessed if tumor cells could uptake EVs released from nontumor cells. B16 melanoma cells that express the Cre-LoxP reporter were injected into B6 mice that ubiquitously expressed Cre. Interestingly, tumor cells with changed phenotype due to the uptake of Cre derived from EVs released from nontumor cells were found sporadically. Therefore, B16 melanoma cells render the ability to take up EVs from healthy cells; however, this transfer does not seem to happen in the same extent as the opposite does. Further studies demonstrated that less malignant tumor cells located either in the same or within distant tumors took up EVs released by tumor cells. In addition, gene expression arrays lead to the discovery of a differential mRNA profile with a significant enrichment of mRNA molecules involved in migration and metastasis in EVs compared to the cells, both of which promote tumor progression. Overall, data suggest that malignant tumor cells, through transfer of EVs, increase migration and metastatic capacity of less malignant cells *in vivo*. Importantly, it was the first time that the transfer of functional cargo through EVs was shown *in vivo*, demonstrating their biological role. This approach is versatile once it can be used in nearly all cell types and more importantly the *in vivo* application allows to study the exchange of EVs in a more natural context, one where cells interact and respond to multiple stimulus of different cell types [50]. Nevertheless, this new strategy is not exosomes specific. Therefore, an *in vivo* model that presents itself as closer to the normal biological system, enabling the study of exosomes natural fate and biological function is still missing.

6. Concluding remarks

Collectively, exosomes spatiotemporal distribution is still elusive, mostly because *in vivo* exosomes research relies on their purification from cells in culture and *in vitro* treatment of other cultured cells or *in vivo* administration in tumor-bearing mice. Despite latest findings, results from *in vitro* experiments cannot be directly extrapolated to the *in vivo* context and need to be carefully analyzed, as clearly pointed by Zomer et al. [50]. Thus far this artificial approach has not given us insight of the actual communication routes of exosomes in the organism, highlighting the great demand for improved animal models that allow exosomes studies *in vivo*. Genetically engineered mouse models (GEMM) could be a promising approach to address the current technical limitations faced. Ideally, these models should allow tracing tumor-derived exosomes while retaining the animal immune system. This important modulator of tumor development is most of the times inexistent since the majority of the experiments are performed using immune deficient mice. Exosomes derived both from tumor and normal cells are known to modulate the immune response as well as the cellular physiology in the tumor surroundings, contributing to a

favorable and permissive microenvironment for the establishment of the tumor and potentially spread to other parts of the organism [52, 53]. It would be very useful to track tumor-derived exosomes in a well-established cancer GEMM model by using an exosomes marker that is fused to a fluorescent protein. Since GFP, RFP and CFP transgenic nude mice appear to have a life span similar to that of non-transgenic nude mice, fluorescent proteins are considered nontoxic and are a promising method for *in vivo* imaging [54]. The scientific community would greatly benefit from these animal models that mimic the best way possible the natural physiology of such a complex disease. Despite intensive efforts, many questions remain unanswered in the field of extracellular vesicles, which the answer could revolutionize today's view both of the normal organism physiology as well as in a cancer context.

Acknowledgements

SAM laboratory is supported by the project NORTE-01-0145-FEDER-000029, supported by Norte Portugal Regional Programme (NORTE 2020), under the PORTUGAL 2020 Partnership Agreement, through the European Regional Development Fund (ERDF) and FEDER funds through the COMPETE Program (POCI-01/0145-FEDER-016618), national funds from FCT – Foundation for Science and Technology PTDC/BIM-ONC/2754/2014 and Maratonas da Saúde. SAM is supported by FCT – Foundation for Science and Technology (IF/00543/2013). We thank Dr. Nuno Barros for the help with the design of the figures included in this chapter.

Author details

Bárbara Adem[1,2] and Sónia A. Melo[1,2,3]*

*Address all correspondence to: smelo@ipatimup.pt

1 Institute for Research and Innovation in Health (i3S), University of Porto, Portugal, Porto, Portugal

2 Institute of Molecular Pathology & Immunology of the University of Porto (IPATIMUP), Porto, Portugal

3 Medical Faculty of the University of Porto, Porto, Portugal

References

[1] Kalluri R. The biology and function of exosomes in cancer. The Journal of Clinical Investigation. 2016;**126**(4):1208-1215

[2] Colombo M, Raposo G, Thery C. Biogenesis, secretion, and intercellular interactions of exosomes and other extracellular vesicles. Annual Review of Cell and Developmental Biology 2014;**30**:255-289

[3] Yang S, et al. Detection of mutant KRAS and TP53 DNA in circulating exosomes from healthy individuals and patients with pancreatic cancer. Cancer Biology & Therapy. 2017

[4] Skog J, et al. Glioblastoma microvesicles transport RNA and proteins that promote tumour growth and provide diagnostic biomarkers. Nature Cell Biology. 2008;**10**(12):1470-1476

[5] Valadi H, et al. Exosome-mediated transfer of mRNAs and microRNAs is a novel mechanism of genetic exchange between cells. Nature Cell Biology. 2007;**9**(6):654-659

[6] Melo SA, et al. Cancer exosomes perform cell-independent microRNA biogenesis and promote tumorigenesis. Cancer Cell. 2014;**26**(5):707-721

[7] Baglio SR, et al. Blocking tumor-educated MSC paracrine activity halts osteosarcoma progression. Clinical Cancer Research. 2017. [Epub ahead of print]

[8] Peinado H, et al. Melanoma exosomes educate bone marrow progenitor cells toward a pro-metastatic phenotype through MET. Nature Medicine. 2012;**18**(6):883-891

[9] Wen SW, et al. The biodistribution and immune suppressive effects of breast cancer–derived exosomes. Cancer Research. 2016;**76**(23):6816

[10] Hood JL, San RS, Wickline SA. Exosomes released by melanoma cells prepare sentinel lymph nodes for tumor metastasis. Cancer Research. 2011;**71**(11):3792

[11] Costa-Silva B, et al. Pancreatic cancer exosomes initiate pre-metastatic niche formation in the liver. Nature Cell Biology. 2015;**17**(6):816-826

[12] Hoshino A, et al. Tumour exosome integrins determine organotropic metastasis. Nature. 2015;**527**(7578):329-335

[13] Wiklander OPB, et al. Extracellular vesicle in vivo biodistribution is determined by cell source, route of administration and targeting. Journal of Extracellular Vesicles. 2015;**4**(1)

[14] Lai CP, et al. Dynamic biodistribution of extracellular vesicles in vivo using a multimodal imaging reporter. ACS Nano. 2014;**8**(1):483-494

[15] Sun D, et al. A novel nanoparticle drug delivery system: The anti-inflammatory activity of curcumin is enhanced when encapsulated in exosomes. Molecular Therapy. 2010;**18**(9):1606-1614

[16] Takahashi Y, et al. Visualization and in vivo tracking of the exosomes of murine melanoma B16-BL6 cells in mice after intravenous injection. Journal of Biotechnology. 2013; **165**(2):77-84

[17] Santos EB, et al. Sensitive in vivo imaging of T cells using a membrane-bound Gaussia princeps luciferase. Nature Medicine. 2009;**15**(3):338-344

[18] Delcayre A, et al. Exosome display technology: Applications to the development of new diagnostics and therapeutics. Blood Cells, Molecules, and Diseases 2005;**35**(2):158-168

[19] Imai T, et al. Macrophage-dependent clearance of systemically administered B16BL6-derived exosomes from the blood circulation in mice. Journal of Extracellular Vesicles. 2015;**4**:26238. DOI:10.3402/jev.v4.26238

[20] Morishita M, et al. Quantitative analysis of tissue distribution of the B16BL6-derived exosomes using a streptavidin-lactadherin fusion protein and iodine-125-labeled biotin derivative after intravenous injection in mice. Journal of Pharmaceutical Sciences. 2015;**104**(2):705-713

[21] Hwang DW, et al. Noninvasive imaging of radiolabeled exosome-mimetic nanovesicle using 99mTc-HMPAO. Scientific Reports 2015,**5**:15636

[22] Phillips WT, Goins BA, Bao A. Radioactive liposomes. Wiley Interdisciplinary Reviews. Nanomedicine and Nanobiotechnology. 2009;**1**(1):69-83

[23] Jang SC, et al. Bioinspired exosome-mimetic nanovesicles for targeted delivery of chemotherapeutics to malignant tumors. ACS Nano. 2013;**7**(9):7698-7710

[24] Varga Z, et al. Radiolabeling of extracellular vesicles with (99m)Tc for quantitative in vivo imaging studies. Cancer Biotherapy and Radiopharmaceuticals. 2016;**31**(5):168-173

[25] Egli A, et al. Organometallic 99mTc-aquaion labels peptide to an unprecedented high specific activity. Journal of Nuclear Medicine. 1999;**40**(11):1913-1917

[26] Hu L, Wickline SA, Hood JL. Magnetic resonance imaging of melanoma exosomes in lymph nodes. Magnetic Resonance in Medicine. 2015;**74**(1):266-271

[27] Busato A, et al. Magnetic resonance imaging of ultrasmall superparamagnetic iron oxide-labeled exosomes from stem cells: A new method to obtain labeled exosomes. International Journal of Nanomedicine 2016;**11**:2481-2490

[28] Bull E, et al. Stem cell tracking using iron oxide nanoparticles. International Journal of Nanomedicine 2014;**9**:1641-1653

[29] Alam SR, et al. Vascular and plaque imaging with ultrasmall superparamagnetic particles of iron oxide. Journal of Cardiovascular Magnetic Resonance. 2015;**17**(1):83

[30] Malatesta M, et al. Diaminobenzidine photoconversion is a suitable tool for tracking the intracellular location of fluorescently labelled nanoparticles at transmission electron microscopy. European Journal of Histochemistry : EJH. 2012;**56**:e20. DOI: 10.4081/ejh.2012.20

[31] Kahlert C, et al. Identification of double stranded genomic DNA spanning all chromosomes with mutated KRAS and p53 DNA in the serum exosomes 7of patients with pancreatic cancer. Journal of Biological Chemistry. 2014;**289**(7):3869-75

[32] Ullal AJ, Pisetsky DS, Reich CF, 3rd. Use of SYTO 13, a fluorescent dye binding nucleic acids, for the detection of microparticles in in vitro systems. Cytometry. Part A. 2010; **77**(3):294-301

[33] Parish CR, Fluorescent dyes for lymphocyte migration and proliferation studies. Immunology and Cell Biology. 1999;**77**(6):499-508

[34] Alvarez-Erviti L, et al. Delivery of siRNA to the mouse brain by systemic injection of targeted exosomes. Nature Biotechnology. 2011;**29**(4):341-345

[35] Zech D, et al. Tumor-exosomes and leukocyte activation: An ambivalent crosstalk. Cell Communication and Signaling. 2012;**10**(1):37

[36] Tian T, et al. Dynamics of exosome internalization and trafficking. Journal of Cellular Physiology. 2013;**228**(7):1487-1495

[37] Tian T, et al. Visualizing of the cellular uptake and intracellular trafficking of exosomes by live-cell microscopy. Journal of Cellular Biochemistry. 2010;**111**(2):488-496

[38] Di Rocco G, Baldari S, Toietta G. Towards therapeutic delivery of extracellular vesicles: Strategies for in vivo tracking and biodistribution analysis. Stem Cells International 2016;**2016**:12

[39] Lai CP, et al. Visualization and tracking of tumour extracellular vesicle delivery and RNA translation using multiplexed reporters. Nature Communications. 2015;**6**:7029

[40] Grange C, et al. Biodistribution of mesenchymal stem cell-derived extracellular vesicles in a model of acute kidney injury monitored by optical imaging. International Journal of Molecular Medicine. 2014;**33**(5):1055-1063

[41] Temchura VV, et al. Enhancement of immunostimulatory properties of exosomal vaccines by incorporation of fusion-competent G protein of vesicular stomatitis virus. Vaccine. 2008;**26**(29-30):3662-3672

[42] Gray WD, Mitchell AJ, Searles CD. An accurate, precise method for general labeling of extracellular vesicles. MethodsX. 2015;**2**:360-367

[43] Gray WD, et al. Identification of therapeutic covariant microRNA clusters in hypoxia-treated cardiac progenitor cell exosomes using systems biology. Circulation Research. 2015;**116**(2):255

[44] Mitchell PJ, et al. Can urinary exosomes act as treatment response markers in prostate cancer? Journal of Translational Medicine. 2009;**7**(1):4

[45] Jiang Y, Li Y, Zhu B. T-cell exhaustion in the tumor microenvironment. Cell Death & Disease. 2015;**6**(6):e1792

[46] Smyth T, et al. Biodistribution and delivery efficiency of unmodified tumor-derived exosomes. Journal of Controlled Release: Official Journal of the Controlled Release Society. 2015;**199**:145-155

[47] Andreu Z, Yáñez-Mó M. Tetraspanins in extracellular vesicle formation and function. Frontiers in Immunology 2014;**5**:442

[48] Suetsugu A, et al. Imaging exosome transfer from breast cancer cells to stroma at metastatic sites in orthotopic nude-mouse models. Advanced Drug Delivery Reviews. 2013;**65**(3):383-390

[49] Amano T, et al. Dynamics of intracellular granules with CD63-GFP in rat basophilic leukemia cells. Journal of Biochemistry. 2001;**129**(5):739-744

[50] Zomer A, et al. Studying extracellular vesicle transfer by a Cre-loxP method. Nature Protocols. 2016;**11**(1):87-101

[51] Zomer A, et al. In vivo imaging reveals extracellular vesicle-mediated phenocopying of metastatic behavior. Cell. 2015;**161**(5):1046-1057

[52] Webber J, et al. Cancer exosomes trigger fibroblast to myofibroblast differentiation. Cancer Research. 2010;**70**(23):9621

[53] Thery C, Ostrowski M, Segura E. Membrane vesicles as conveyors of immune responses. Nature Reviews. Immunology. 2009;**9**(8):581-593

[54] Hoffman RM. Application of GFP imaging in cancer. Laboratory Investigation; A Journal of Technical Methods and Pathology. 2015;**95**(4):432-452